

Adaptive Group Sparse Regularization for Continual Learning

Sangwon Jung¹, Hongjoon Ahn², Sungmin Cha¹ and Taesup Moon^{1,2}

¹Department of Electrical and Computer Engineering, ² Department of Artificial Intelligence
Sungkwunkwan University, Suwon, Korea 16419

{s.jung, hong0805, csm9493, tsmoon}@skku.edu

Abstract

We propose a novel regularization-based continual learning method, dubbed as Adaptive Group Sparsity based Continual Learning (AGS-CL), using two group sparsity-based penalties. Our method selectively employs the two penalties when learning each node based its the importance, which is adaptively updated after learning each new task. By utilizing the proximal gradient descent method for learning, the exact sparsity and freezing of the model is guaranteed, and thus, the learner can explicitly control the model capacity as the learning continues. Furthermore, as a critical detail, we re-initialize the weights associated with unimportant nodes after learning each task in order to prevent the negative transfer that causes the catastrophic forgetting and facilitate efficient learning of new tasks. Throughout the extensive experimental results, we show that our AGS-CL uses much less additional memory space for storing the regularization parameters, and it significantly outperforms several state-of-the-art baselines on representative continual learning benchmarks for both supervised and reinforcement learning tasks.

1. Introduction

Continual learning, also referred to as lifelong learning, is a long standing open problem in machine learning, in which the training dataset is given sequentially in a form divided into the groups of tasks. The goal of continual learning is to adapt quickly to the incoming tasks and not forget about the previously learned tasks. However, there is a fundamental tradeoff that needs to be overcome: the *stability-plasticity dilemma* [5, 20]. This means that if the artificial neural network(ANN)-based model focuses too much on remembering the already learned tasks, it will have difficulty in learning a new task, while if the model focuses too much on adapting to a new task, it loses the information of the learned task and suffers from the *catastrophic forgetting*. In contrast to ANNs, humans can maintain the information of the previously learned task well enough while learning a new

task, and even when the forgetting happens, the information of the learned tasks can be unknowingly managed in the form of *gracefully forgetting*.

To overcome this fundamental difference between human beings and ANNs, a comprehensive study for ANN-based continual learning was conducted broadly under the following three categories. Firstly, dual memory system-based methods [24, 19, 30, 11] maintain additional memory such that it can store some representative data used to learn the previous tasks and use them when learning a new task. Secondly, dynamic network architecture-based methods [25, 35, 8] append or eliminate weights in the network as the learning happens with the continually arriving task data. Finally, the regularization-based methods [17, 13, 36, 21, 1] identify important learned weights for previous tasks and heavily penalize their deviation while learning new tasks. Among above three categories, we focus on the regularization-based methods, since they pursue to use the neural network as efficiently as possible in the continual learning setting and have a potential to get combined with other approaches to bring the synergy.

The regularization-based continual learning methods have a natural connection with a separate line of research, the model compression [16, 18, 37]. Namely, in order to obtain a compact model, typical model compression methods measure the importance of each node or weight in a given neural network and prune the unimportant ones. Several representative methods [33, 3, 34, 26] used the group Lasso-like penalties, which define the incoming or outgoing weights to a *node* as groups, and achieve structured sparsity within a neural network to compress the network. Such focus on the node-level importance could lead to more efficient representation of the model and showed better performance than focusing on the weight-wise importance. In continual learning, a similar spirit of considering the importance of *nodes*, instead of *weights*, has been considered as well. For instance, [29] and [1] attained the node-wise importance assignment via utilizing attention mechanism and Bayesian inference, respectively, but without any exact sparsification or freezing of a model. In contrast, [8] explicitly achieved exact sparsity

or freezing of a model, but via cumbersome threshold tuning for the pruning steps.

In this paper, we propose a new regularization-based continual learning method, dubbed as Adaptive Group Sparsity based Continual Learning (AGS-CL), using *two* group sparsity-based penalties as novel regularization terms. The two terms are designed to deal with the stability-plasticity dilemma and attain the exact node-wise sparsification and freezing in an *adaptive* and *automatic* manner, unlike the previous continual learning work [29, 1, 8] mentioned above. Namely, the first term, which is equivalent to the ordinary group Lasso penalty, efficiently assigns and learns new important nodes when learning a new task (*i.e.*, *plasticity*), whereas the second term, which is a group sparsity penalty imposed on the deviation of the important node parameters, prevents the forgetting of the previously learned important nodes via freezing the incoming weights to the nodes (*i.e.*, *stability*). The two terms are selectively applied to each node in the model based on the adaptive regularization parameter that represents the *importance* of each node, which is updated after learning each new task. Furthermore, the adaptive regularization parameters are exponentially averaged as the learning continues such that gracefully forgetting of the node importance can be implemented.

For learning, we utilize the proximal gradient descent (PGD) [22] method such that the *exact* sparsity and freezing of the model can be attained, and thus, the explicit control of the model capacity is possible as the learning continues. Moreover, as a critical detail, we implement the re-initializations of the weights associated with the *unimportant* nodes after learning each task, such that the negative transfer, which we believe is one of the main sources of the catastrophic forgetting, can be prevented. As a result, throughout our extensive experiments, we show that our AGS-CL does an excellent job in efficiently mitigating the catastrophic forgetting while continuously learning new tasks for both supervised and reinforcement learning, and it significantly outperforms several strong state-of-the-art baselines, *e.g.*, EWC, SI, and RWALK [13, 36, 6]. Furthermore, we show that using the node-wise regularization parameters in AGS-CL has a nice by-product of significantly saving the additional memory to store the parameters than the other baselines, which have to store the parameter for each *weights*. Such compact memory usage enables applying AGS-CL to much larger networks, which typically is necessary for applications with large-scale datasets.

Following summarizes our key contributions:

- To the best of our knowledge, we first use the group Lasso and group sparsity based regularization terms together with PGD for continual learning.
- We proposed the adaptive regularization parameter, which determines the importance of a node and is used to apply the two regularization terms selectively.
- We achieve the state-of-the-art performance on several continual learning benchmarks, including large-scale supervised learning and reinforcement learning tasks, while using much less additional memory for storing the regularization parameters than other baselines.

2. Related Work

Continual learning There are various research on continual learning conducted for many years, as summarized in [23], and we will only summarize methods that are relevant to our approach. The regularization-based methods identify the important weights or nodes of neural tasks for previous tasks and penalize their deviation relying on their importance while learning a new task. LWF[17] maintains the output layer corresponding to each task and proposes a regularization term that holds the output value of the output layer via distilling knowledge of the previously learned model[10]. EWC[13] calculates the diagonal of the fisher information matrix at the end of learning each task and uses them as the relative importance of the parameters. SI[36] also calculates the importance of the parameter considering the path integral of the gradient vector field. MAS[2] defines the importance of the parameter as the magnitude of the gradient value of the parameter in an unsupervised manner. RWALK[6] is a combined version of SI and EWC, which uses both fisher information and path integral of the gradient vector field. Unlike EWC, SI, MAS and RWALK, in UCL[1], they consider the importance of node as uncertainty of incoming weights which is measured by using variational inference.

There have been a lot of approaches for continual learning other than the regularization-based method. In HAT [29], appending the embedding layer with task identifier, they utilize a node-wise hard attention mechanism per layer which is different from our explicit regularization terms for overcoming catastrophic forgetting. In CLNP[8], although they have a similar motivation with our method in terms of identifying the important nodes for each task by using regularization, they need a manually designed scheme for gracefully forgetting which is tricky threshold tuning for node pruning steps. DEN[35] presented a method of model growing based continual learning that utilizes group Lasso for augmenting the model effectively. Although it is similar to our approach in terms of using group Lasso, we assume the capacity of given models is limited, in contrast to DEN.

Group Lasso A few recent works applied group Lasso regularization to deep neural networks on model compression [3, 33, 34, 26], focusing on sparsification of unimportant nodes for target tasks. [3] proposed an approach to automatically decide the number of neurons and compress an excessively large neural network by using group Lasso. Similarly, in [33], the structure of deep neural networks is directly adjusted through a structured sparsity learning. While they

make use of group sparsity regularization for compression, it can be also considered as a means to efficiently use the capacity of a model for a sequence of tasks, similarly to [35]. We employ the group Lasso regularization for two purposes: sparsification and consolidation. Especially, while most previous regularization based continual learners [13, 36, 2] applied L2 regularizer to remember past tasks, we use group Lasso based regularizer that prevents catastrophic forgetting more surely.

3. Main Method

3.1. Motivation

Here, we give the main motivation for our algorithm. While several state-of-the-art baselines, [13, 36, 6], considered the weight-level importance for devising the regularization terms, we believe that working with the node-level importance is more sensible and effective since the node is the basic unit for representing the learned information from a task. Such approach also has a benefit of saving additional memory for storing the regularization parameters, and it has been adopted in recent work [29, 1, 8] as well. Since identifying important nodes while training a neural network model is exactly what is done in the group Lasso-based model compression methods [33, 3, 34, 26], we adopt the same methodology for compactly identifying important nodes when continuously learning new tasks.

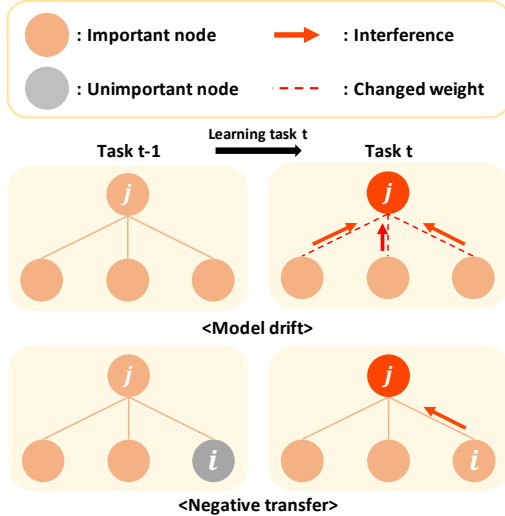


Figure 1. Two sources of catastrophic forgetting: *model drift* (top) and *negative transfer* (bottom). The role of the red node, which was identified as important for task $t - 1$, inevitably alters when either its incoming weights change (model drift) or unimportant node in the lower layer becomes important (negative transfer) while learning a new task t .

Assuming the important nodes for task $t - 1$ are identified, we argue that there are two sources for the catastrophic forgetting as the learning continues with new tasks: *model*

drift and *negative transfer* as shown in Figure 1. The model drift corresponds to the case in which the incoming weights of a node that was important for task $t - 1$ (node j in Figure 1(top)) gets changed when learning a new task t . In this case, the representation of node j for task $t - 1$ can alter, hence, the performance for task $t - 1$ can drastically degrade, leading to the catastrophic forgetting. The red arrows and dotted lines in the figure exemplify such model drift for node j . On the other hand, the negative transfer happens when the representation of an unimportant node for task $t - 1$ in the lower layer (node i in Figure 1(bottom)) changes during learning a new task t . Namely, even when there is no model drift, if node i becomes important for task t , then such change of representation will bring an interfering effect for node j when carrying out task $t - 1$. The color change of i and red arrow in the figure exemplifies such negative transfer from the future tasks.

In order to address above two key sources of catastrophic forgetting, we believe an effective continual learning algorithm should essentially carry out the following two:

- *Freeze important nodes*: Once a node has been identified as important, its *incoming* weights should be frozen while learning future tasks, such that the *model drift* can be prevented.
- *Prevent negative transfer*: When a node has been identified as unimportant, its *outgoing* weights should be fixed to 0, such that the *negative transfer* from the node to the upper layers can be eliminated when the node becomes important for future tasks.

We note the processes similar to above also appear in [8], but they do explicit pruning and freezing of the model weights based on cumbersome hyperparameter tuning and using a separate validation set. Our proposed AGS-CL instead automatically determines the important and unimportant nodes as the learning continues, freezes the incoming weights for the important ones, and zeroes the outgoing weights for the unimportant ones, all via selectively applying two group sparsity based penalties based on the adaptive regularization parameter for each node.

3.2. Notations

We denote $\ell \in \{1 \dots, L\}$ as a layer of a neural network model that has N_ℓ nodes, and let $n_\ell \in \{1, \dots, N_\ell\}$ be a node in that layer. For the convolutional neural networks (CNN), the node stands for the convolution channel. Moreover, θ_{n_ℓ} denotes the vector of the (incoming) weight parameters for the n_ℓ -th node. Hence, $\theta_{n_\ell, i}$ stands for the weight that connects the i -th node (or channel) in layer $\ell - 1$ with the node n_ℓ . Moreover, $\mathcal{G} \triangleq \{n_\ell : 1 \leq n_\ell \leq N_\ell, 1 \leq \ell \leq L\}$ is the set of all the nodes in the neural network, and $\theta = \{\theta_{n_\ell}\}_{n_\ell \in \mathcal{G}}$ denotes the entire parameter vector of the network. In our continual learning setting, $\mathcal{D}_t = \{(\mathbf{x}_m^{(t)}, y_m^{(t)})\}_{m=1}^{N_t}$ stands for the training dataset for task $t \in \{1, \dots, \mathcal{T}\}$, and we

assume the task boundaries are given to the learner.

Following [22], we denote the proximal operator as

$$\text{prox}_{\alpha f}(\mathbf{v}) = \arg \min_{\boldsymbol{\theta}} \left(f(\boldsymbol{\theta}) + \frac{1}{2\alpha} \|\boldsymbol{\theta} - \mathbf{v}\|_2^2 \right) \quad (1)$$

for a scalar $\alpha > 0$ and a convex function f . We heavily use the proximal operator in learning the network parameters with the group sparsity based regularizers.

3.3. Adaptive Group Sparse Regularization

3.3.1 Loss function

Before describing our loss function, we first introduce the *adaptive* regularization parameter $\Omega_{n_\ell}^{(t-1)} \geq 0$ for each node $n_\ell \in \mathcal{G}$, of which magnitude indicates how important the node is for carrying out the task up to $t - 1$. Namely, large $\Omega_{n_\ell}^{(t-1)}$ indicates that the node n_ℓ has been identified and learned as important for learning up to task $t - 1$, and if $\Omega_{n_\ell}^{(t-1)} = 0$, then the node n_ℓ was *not* important for learning tasks up to $t - 1$. The exact definition and update mechanism for $\Omega_{n_\ell}^{(t-1)}$ are given in Section 3.3.3, but for now, we assume such parameter is given when learning a new task t . Now, given the regularization parameters $\{\Omega_{n_\ell}^{(t-1)}\}_{n_\ell \in \mathcal{G}}$, we can define a set of unimportant nodes,

$$\mathcal{G}_0^{(t-1)} \triangleq \{n_\ell : \Omega_{n_\ell}^{(t-1)} = 0\} \subseteq \mathcal{G}. \quad (2)$$

With above definitions and given the training data \mathcal{D}_t , our loss function for learning task t is then set as

$$\mathcal{L}_t(\boldsymbol{\theta}) = -\frac{1}{N_t} \sum_{m=1}^{N_t} \log p(y_m^{(t)} | \mathbf{x}_m^{(t)}; \boldsymbol{\theta}) \quad (3)$$

$$+ \mu \sum_{n_\ell \in \mathcal{G}_0^{(t-1)}} \|\boldsymbol{\theta}_{n_\ell}\|_2 \quad (4)$$

$$+ \lambda \sum_{n_\ell \in \mathcal{G} \setminus \mathcal{G}_0^{(t-1)}} \Omega_{n_\ell}^{(t-1)} \|\boldsymbol{\theta}_{n_\ell} - \hat{\boldsymbol{\theta}}_{n_\ell}^{(t-1)}\|_2, \quad (5)$$

in which (3) is the ordinary cross-entropy loss function on the training data, $\hat{\boldsymbol{\theta}}_{n_\ell}^{(t-1)}$ is the learned parameter for node n_ℓ up to task $t - 1$, and $\mu \geq 0$ and $\lambda \geq 0$ are the hyperparameters that set the trade-offs among the loss terms. Notice that our loss function *adaptively* employs the group-sparsity based regularization terms based on the value of $\Omega_{n_\ell}^{(t-1)}$. Namely, for the unimportant nodes in $\mathcal{G}_0^{(t-1)}$, we apply the ordinary group Lasso regularization (4) as in [3], and for the important nodes in $\mathcal{G} \setminus \mathcal{G}_0^{(t-1)}$, we apply the group-sparsity based penalty (5) that adaptively penalizes the deviation of $\boldsymbol{\theta}_{\ell,n}$ from the previously learned $\hat{\boldsymbol{\theta}}_{\ell,n}^{(t-1)}$ depending on the magnitude of $\Omega_{n_\ell}^{(t-1)} > 0$. Such adaptive penalization resembles those of adaptive Lasso [38] or adaptive group Lasso [31].

We elaborate that minimizing $\mathcal{L}_t(\boldsymbol{\theta})$ naturally incorporates the efficient active learning of a new task (*i.e.*, plasticity) and freezing important nodes for past tasks to prevent the *model drift* mentioned in Section 3.1 (*i.e.*, stability). Namely, the group Lasso term (4) automatically identifies the active learners for the new task t from the nodes identified as unimportant so far (*i.e.*, those in $\mathcal{G}_0^{(t-1)}$), and *sparsify* the rest of the nodes such that they can be allocated for learning future tasks. Furthermore, the penalty term (5) enforces to *freeze* $\boldsymbol{\theta}_{n_\ell}$ to $\hat{\boldsymbol{\theta}}_{n_\ell}^{(t-1)}$ when a node has been identified to be important enough, *i.e.*, it has large $\Omega_{n_\ell}^{(t-1)}$ value. Note due to the property of the group-norm penalties, the sparsification and freezing resulting from the two terms can be *exact* when appropriate optimization method is used, as described in the next subsection.

3.3.2 Learning with proximal gradient descent

While directly minimizing our loss $\mathcal{L}_t(\boldsymbol{\theta})$ can be done via using vanilla SGD-variant optimizers, *e.g.*, Adam [12], we utilize the proximal gradient descent (PGD) method [22, Section 4.2] to induce the *exact* freezing and sparsifying of the nodes after the minimization is done.

Note our loss function can be written as

$$\mathcal{L}_t(\boldsymbol{\theta}) = \mathcal{L}_{\text{CE}}(\boldsymbol{\theta}) + \mathcal{L}_{\text{Reg}}(\boldsymbol{\theta}), \quad (6)$$

in which $\mathcal{L}_{\text{CE}}(\boldsymbol{\theta})$ is the data loss (3) and $\mathcal{L}_{\text{Reg}}(\boldsymbol{\theta})$ is the *convex* regularization term that combines (4) and (5). The proximal gradient descent method with learning rate α then iteratively minimizes (6) by computing

$$\tilde{\boldsymbol{\theta}}^{k+1} := \boldsymbol{\theta}^k - \alpha \nabla \mathcal{L}_{\text{CE}}(\boldsymbol{\theta}^k) \quad (7)$$

$$\boldsymbol{\theta}^{k+1} := \text{prox}_{\alpha \mathcal{L}_{\text{Reg}}(\boldsymbol{\theta})}(\tilde{\boldsymbol{\theta}}^{k+1}) \quad (8)$$

in which $\boldsymbol{\theta}^k$ is the k -th proximal gradient update step. Namely, in words, (8) applies the proximal operator (1) with $f = \mathcal{L}_{\text{Reg}}(\boldsymbol{\theta})$ on the gradient update of $\boldsymbol{\theta}^k$ using $\nabla \mathcal{L}_{\text{CE}}(\boldsymbol{\theta}^k)$.

Now, for a succinct, concrete update rule for our algorithm, we introduce the following lemma.

Lemma 1 For $f(\boldsymbol{\theta}) = c\|\boldsymbol{\theta} - \boldsymbol{\theta}_0\|_2$ with $c > 0$ and any fixed vector $\boldsymbol{\theta}_0$,

$$\text{prox}_{\alpha f}(\mathbf{v}) = \gamma \mathbf{v} + (1 - \gamma) \boldsymbol{\theta}_0, \quad (9)$$

in which

$$\gamma = \left(1 - \frac{\alpha c}{\|\boldsymbol{\theta}_0 - \mathbf{v}\|_2} \right)_+ \quad (10)$$

where $(x)_+ = \max\{0, x\}$.

From (1), we can easily see that the proximal operator can be applied to each node parameter vector $\boldsymbol{\theta}_{n_\ell}$ independently when carrying out (8). Hence, by Lemma 1, we have the following closed-form proximal gradient update rules:

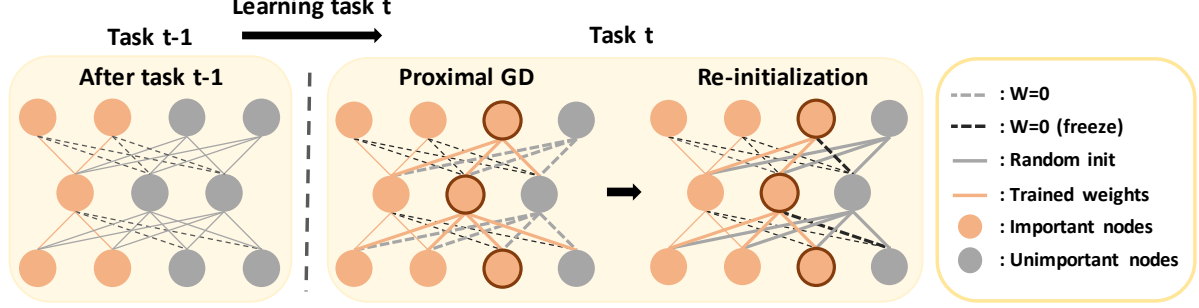


Figure 2. Summary of our AGS-CL. During learning a new task t , the PGD step using term (4) identifies the *new* important nodes (orange nodes with red boundaries) and remaining unimportant nodes (gray nodes with bold, dotted weights). The incoming weights connected to the important nodes up to $t-1$ (vanilla orange nodes) are frozen at t due to the PGD step with (5). The re-initialization step then fixes the outgoing weights of unimportant nodes to zero (the bold, black dotted lines) and randomly initializes the incoming weights for nodes in $\{n_\ell : \|\hat{\theta}_{n_\ell}^{(t)}\|_2 = 0\}$ (bold gray solid lines).

- For $n_\ell \in \mathcal{G}_0^{(t-1)}$,

$$\theta_{n_\ell}^{k+1} := \left(1 - \frac{\alpha\mu}{\|\tilde{\theta}_{n_\ell}^k\|_2}\right)_+ \tilde{\theta}_{n_\ell}^k, \quad (11)$$

- For $n_\ell \in \mathcal{G} \setminus \mathcal{G}_0^{(t-1)}$,

$$\theta_{n_\ell}^{k+1} := \gamma \tilde{\theta}_{n_\ell}^k + (1 - \gamma) \hat{\theta}_{n_\ell}^{(t-1)} \quad (12)$$

with

$$\gamma = \left(1 - \frac{\alpha\lambda\Omega_{n_\ell}^{(t-1)}}{\|\tilde{\theta}_{n_\ell}^k - \hat{\theta}_{n_\ell}^{(t-1)}\|_2}\right)_+. \quad (13)$$

Note (11) can set $\theta_{n_\ell}^{k+1} = \mathbf{0}$ (i.e., sparsifying) when $\|\tilde{\theta}_{n_\ell}^k\|_2 \leq \alpha\mu$, and (12) can set $\theta_{n_\ell}^{k+1} = \hat{\theta}_{n_\ell}^{(t-1)}$ (i.e., freezing) when $\|\tilde{\theta}_{n_\ell}^k - \hat{\theta}_{n_\ell}^{(t-1)}\|_2 \leq \alpha\lambda\Omega_{n_\ell}^{(t-1)}$. Thus, we can obtain the *exact* pruning and freezing for the unimportant and important nodes, respectively, as we intended and described in Section 3.3.1. Moreover, from the theory of proximal gradient descent, the update rules of (11) and (12) will converge to a local minima of $\mathcal{L}_t(\theta)$ with appropriate learning rate α . The converged parameters after learning task t are then denoted as $\hat{\theta}^{(t)} = \{\hat{\theta}_{n_\ell}^{(t)}\}_{n_\ell \in \mathcal{G}}$.

3.3.3 Updating $\Omega_{n_\ell}^{(t-1)}$ and re-initialization

As described in Section 3.3.1, the adaptive regularization parameters $\{\Omega_{n_\ell}^{(t-1)}\}_{n_\ell \in \mathcal{G}}$ reflect the importance of nodes and play a crucial role in our loss function and learning. The definition and the update formula for the parameters are as described below.

Initially, we set $\Omega_{n_\ell}^{(0)} = 0$ for all $n_\ell \in \mathcal{G}$, and thus, for $t = 1$, we obtain the ordinary group Lasso solution since $\mathcal{G}_0^{(0)} = \mathcal{G}$. After the minimization of $\mathcal{L}_t(\theta)$ is done, the regularization parameters get updated as

$$\Omega_{n_\ell}^{(t)} := \eta \Omega_{n_\ell}^{(t-1)} + \frac{1}{N_t} \sum_{m=1}^{N_t} a_{n_\ell}(\mathbf{x}_m^{(t)}), \quad (14)$$

in which $a_{n_\ell}(\mathbf{x}_m^{(t)})$ is the ReLU activation value of the node n_ℓ when the input data is $\mathbf{x}_m^{(t)} \in \mathcal{D}_t$ and $0 < \eta \leq 1$ is the hyperparameter for exponential averaging. Hence, the average activation value of n_ℓ for task t is regarded as the *importance* of the node and added to $\Omega_{n_\ell}^{(t-1)}$. Note when $\eta < 1$, the gracefully forgetting of $\Omega_{n_\ell}^{(t-1)}$ can be done, similarly as the online EWC in [28], such that the level of node freezing by PGD within a fixed network capacity is controlled.

Once $\{\Omega_{n_\ell}^{(t)}\}_{n_\ell \in \mathcal{G}}$ are updated, we carry out two re-initialization steps on the weights that are connected to the unimportant nodes that are in $\mathcal{G}_0^{(t)}$. Such re-initializations are the critical steps for preventing the *negative transfer* and enabling *effective learning* for learning future tasks. That is, for the learned weights $\hat{\theta}^{(t)} = \{\hat{\theta}_{n_\ell}^{(t)}\}_{n_\ell \in \mathcal{G}}$, we do

(I.1) Fix $\hat{\theta}_{n_\ell, i}^{(t)} = 0$ if $i \in \mathcal{G}_0^{(t)}$.

(I.2) Rand-Init($\hat{\theta}_{n_\ell}^{(t)}$) if $n_\ell \in \{n_\ell : \|\hat{\theta}_{n_\ell}^{(t)}\|_2 = 0\} \subseteq \mathcal{G}_0^{(t)}$.

The former fixes the *outgoing* weights of an unimportant node in $\mathcal{G}_0^{(t)}$ to zero during *all* remaining tasks, while the latter randomly initializes the *incoming* weight vector of an unimportant node that has norm 0.

The intuitions of the two steps are the following. Firstly, we can see from (14) that $\Omega_i^{(t)} = 0$ implies $\Omega_i^{(t-1)} = 0$ and $a_i(\mathbf{x}_m^{(t)}) = 0$ for all $\mathbf{x}_m \in \mathcal{D}_t$ for a node $i \in \mathcal{G}_0^{(t)}$. Hence, when $i \in \mathcal{G}_0^{(t)}$, it was unimportant for task $t-1$, and *never* gets activated for data in \mathcal{D}_t after learning task t , thus, still remains unimportant. Thus, by (I.1), we can prevent the negative transfer of the case depicted in Figure 1 since the change of the representation of the unimportant node will never affect the important nodes connected to it. Secondly, we note $\mathcal{G}_0^{(t)} = \{n_\ell : \|\hat{\theta}_{n_\ell}^{(t)}\|_2 = 0\} \cup \{n_\ell : \|\hat{\theta}_{n_\ell}^{(t)}\|_2 > 0, \sum_{m=1}^{N_t} a_{n_\ell}(\mathbf{x}_m) = 0\}$, and the incoming weights of the nodes in the first set would suffer from the vanishing gradient problem while training the new task after t . Hence, by randomly initializing those weights, we enable the nodes to potentially become active learners for the future tasks. In our

Algorithm 1 AGS-CL algorithm

Require: $\{\mathcal{D}_t\}_{t=1}^T$: Sequential training datasets
Require: μ, λ : Hyperparameters, \mathcal{K} : the number of mini-batch iterations for each task
Randomly initialize θ and set $\Omega_{n_\ell}^{(0)} = 0, \forall n_\ell \in \mathcal{G}$.
for $t = 1, \dots, T$ **do**
 for $k = 1, \dots, \mathcal{K}$ **do**
 /* Proximal gradient descent */
 Compute $\tilde{\theta}^k$ as in (7)
 for Each $n_\ell \in \mathcal{G}$ **do**
 Obtain $\theta_{n_\ell}^{k+1}$ using (11) or (12)
 end for
 end for
 Update $\{\Omega_{n_\ell}^{(t)}\}_{n_\ell \in \mathcal{G}}$ using (14)
 Obtain $\mathcal{G}_0^{(t)}$ as in (2)
 /* Re-initialization */
 Re-initialize θ using (I.1) and (I.2)
end for

experimental results, we show the critical effects of these two re-initialization steps. The summary of our algorithm is given in Algorithm 1, and the overall learning mechanism of our method is illustrated in Figure 2.

4. Experimental Results

4.1. Supervised learning on vision datasets

We evaluate the performance of AGS-CL together with the representative regularization-based methods, EWC [13], SI [36], RWALK [6], and HAT [29]. We used multi-headed outputs for all experiments, and 5 different random seed runs are averaged for all datasets. For the experiments with all datasets, we used convolutional neural networks (CNN), of which architectures are the following: for CIFAR10/100 [14], we used 6 convolution layers followed by 2 fully connected layers, for Omniglot[15], as in [28], we used 4 convolution layers, and for CUB200 [32], we used Resnet-18 [9] pre-trained on ImageNet [7] dataset. We fairly searched the hyperparameters for all baselines and report the best performance for each method.

Split CIFAR-100 & CIFAR-10/100 To show the effectiveness on simple benchmark with small number of tasks, we experimented on Split CIFAR-100 and Split CIFAR-10/100 datasets¹. Split CIFAR-100 consists of 10 tasks, of which each task consists of 10 consecutive classes of CIFAR-100. Split CIFAR-10/100 additionally uses CIFAR-10 dataset for pre-training before continually learning CIFAR-100. In two left figures of Figure 3 show the results. In Split CIFAR-100, the average accuracy of EWC and SI are almost the same; 60.1% and 60.3%, respectively, which are slightly bet-

¹We omit the experiments on PMNIST or CIFAR-10 since they turn out to be less challenging.

ter than RWALK and HAT; 58.0% and 59.1%, respectively. We clearly observe our AGS-CL significantly outperforms all of them and achieves 63.0%. In Split CIFAR-10/100, the performance of all baselines, except for HAT, are much higher than those in Split CIFAR-100, and AGS-CL again outperforms all the baselines by achieving 72.5%.

Omniglot To check the competence of dealing with much longer sequence of tasks, we experimented our approach on Omniglot, of which each alphabet is treated as a single task, and we used all 50 alphabets. As in [28], we rescaled all images to 28×28 and did data augmentation by including 20 random permutations (rotations and shifting) for each image. Unlike in Split CIFAR-10 or CIFAR-10/100, each Omniglot task consists of different number of classes, and the total number of classes is almost 1600. The third plot in Figure 3 shows our AGS-CL achieves the average accuracy of 82.5%, which is much higher than all other baselines: EWC (71.6%), RWALK (71.8%) and SI (68.9%). HAT was not comparable. From the curve, we observe AGS-CL hardly suffers from any forgetting, while others show high variations in their accuracy.

CUB200 In order to check the ability of continual learning from a pre-trained large-scale network, we tested on the CUB200, which has 10 tasks with 20 bird classes in each task. For the pre-trained ResNet-18 model, we again initialized $\Omega_{n_\ell}^{(0)} = 0$ and . From the right plot of Figure 3, we again observe that AGS-CL achieves the highest accuracy, 90.5%. Although EWC performs better than SI and RWALK and is similar to AGS-CL, as shown in Figure 6 below, our AGS-CL is much more memory efficient in storing the regularization parameters. Such memory efficiency is much more noticeable especially when using large-scale CNN models like ResNet-18. In addition, HAT could not run on CUB200 dataset.

Analysis 1: Sparsity and used capacity of the model

Here, we closely analyze the pattern of the sparsity and used capacity of the CNN model while continual learning with our AGS-CL. We define the sparsity of a network as the ratio $|\mathcal{G}_0^{(t)}|/|\mathcal{G}|$ and the used capacity as the ratio $|\{n_\ell : \|\hat{\theta}_{n_\ell}^{(t)} - \hat{\theta}_{n_\ell}^{(t-1)}\|_2 = 0\}|/|\mathcal{G}|$. Thus, if the sparsity is large, there are many “active learners”, and if the used capacity is large, most of the nodes are frozen. Figure 4 shows how sparsity and used capacity of the network evolve as the learning continues for Split CIFAR-100. We can observe that as the learning continues, the sparsity gradually decreases and the used capacity gradually increases as desired. Furthermore, we observe that the re-initialization steps in AGS-CL is essential; namely, without the re-initialization, the network sparsity does not drop beyond a certain level, hence, AGS-CL cannot utilize the full capacity of the network.

Analysis 2: Effect of re-initialization on the stability and plasticity

To study how helpful the re-initialization step is to prevent the *negative transfer* and to enable the *effective*

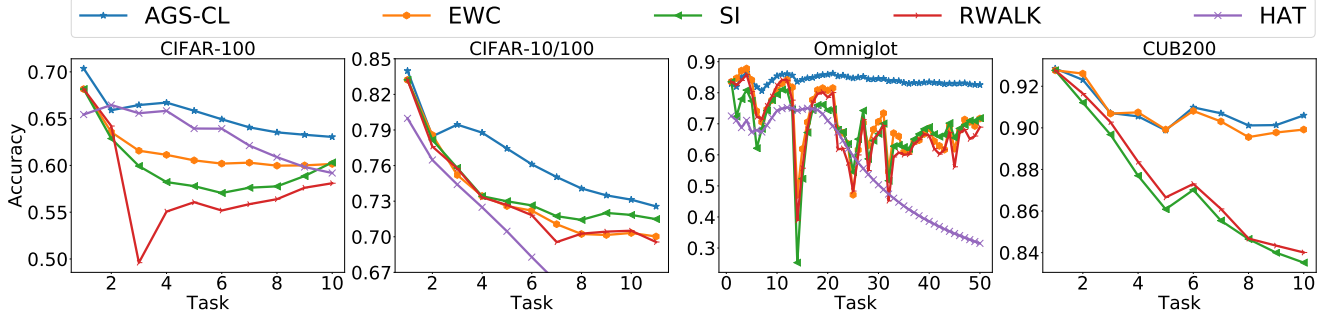


Figure 3. Experiment results on vision dataset.

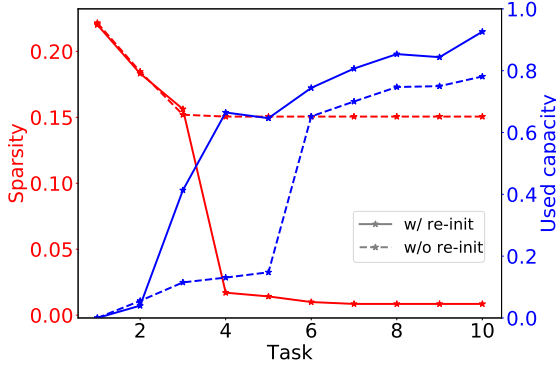


Figure 4. Analysis on network sparsity and used capacity with or without re-initialization for Split CIFAR-100. The left (red) y -axis represents the sparsity and the right (blue) y -axis represents the used capacity. Two types of lines represent whether we apply the re-initialization steps or not.

learning, we evaluated with two additional metrics, *plasticity* and *stability*, which are defined as below.

We let $A \in \mathbb{R}^{\mathcal{T} \times \mathcal{T}}$ be the accuracy matrix of a continual learning algorithm, in which $A_{i,j}$ is the accuracy of the j -th task after learning the i -th task, and let $A^* \in \mathbb{R}^{\mathcal{T} \times \mathcal{T}}$ be the accuracy matrix of a vanilla fine-tuning scheme without any continual learning mechanism. Then, we define the plasticity as

$$\mathcal{P} = \frac{1}{\mathcal{T}} \sum_{i=1}^{\mathcal{T}} \frac{A_{i,i}}{A_{i,i}^*}, \quad (15)$$

and the stability as

$$\mathcal{S} = \frac{1}{\mathcal{T}} \sum_{j=1}^{\mathcal{T}} \frac{A_{\mathcal{T},j}}{\max_{j \leq i \leq \mathcal{T}} (A_{i,j})}. \quad (16)$$

Namely, (15) measures the relative accuracy of the continual learning algorithm for the current task compared to the fine-tuning, *i.e.*, the amount of forward transfer, and (16) measures the relative accuracy of a task after learning all \mathcal{T} tasks to the maximum accuracy for the task throughout the learning process, *i.e.*, the amount of forgetting.

Figure 5 reports the trade-offs of \mathcal{P} and \mathcal{S} , obtained from Split CIFAR-100 for several variants of AGS-CL and EWC. For AGS-CL, we ablated each re-initialization scheme in Section 3.3.3; ‘w/o re-init’ stands for the scheme without any re-initialization, ‘w/o rand-init’ stands for the scheme that only does (I.1), and ‘w/o zero-init’ stands for the scheme that only does (I.2). Moreover, the plotted trade-offs are over the hyperparameters; *i.e.*, for AGS-CL, we fixed μ and varied λ , and for EWC, we varied λ . The two ‘ \star ’ points in the figure represent the results of the optimum λ for AGS-CL (blue) and EWC (black). We can make the following observations from the figure. Firstly, we note AGS-CL shows much better \mathcal{P} - \mathcal{S} trade-off than EWC. Namely, for fixed \mathcal{P} , AGS-CL has better \mathcal{S} , hence, better prevents the negative transfer. Moreover, for fixed \mathcal{S} , AGS-CL has better \mathcal{P} , hence, does efficient learning of new task with active learners. Second, we observe the random initialization, (I.2), is critical particularly for improving \mathcal{P} , since ‘w/o rand-init’ maintains the similar \mathcal{S} as AGS-CL but with significant degradation in \mathcal{P} . Thirdly, we observe the zero-fixing, (I.1), is mainly critical for improving \mathcal{S} , since ‘w/o zero-init’ shows similar \mathcal{P} as AGS-CL, but has drop in \mathcal{S} . This result is in line with our intuition that (I.1) would prevent *negative transfer*. Finally, ‘w/o re-init’ and ‘w/o rand-init’ show similar performance, hence (I.1) alone is not enough for attaining high on both \mathcal{P} and \mathcal{S} .

Analysis 3: Comparison of required memory size Figure 6 shows the relative required memory size for each method. The memory size is the sum of the size of regularization parameters, stored model, and a model currently being trained. The relative memory size is normalized with the memory size of EWC. In Figure 6, we can see that AGS-CL uses much less memory than other regularization-based methods because the size of weight importance matrix in EWC, SI and RWALK is same as the model parameters. However, since AGS-CL uses the node-wise importance, it can reduce the memory size drastically. Though HAT has the smallest number of parameters, the performance is much lower than other baselines.

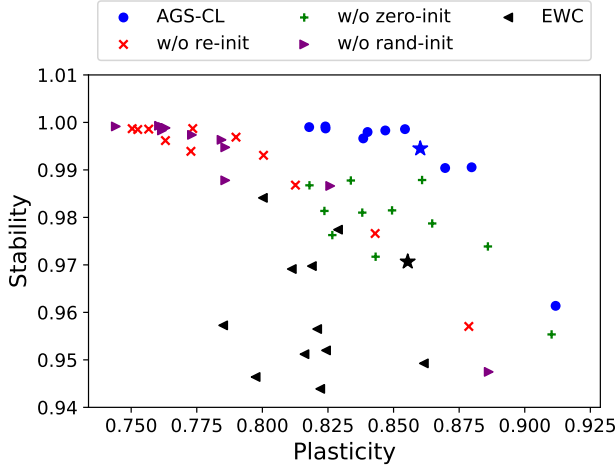


Figure 5. The trade-offs on the plasticity and stability for several variants of AGS-CL and EWC.

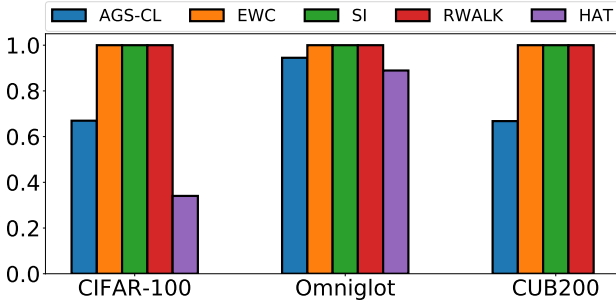


Figure 6. Comparison on the relative required memory size.

4.2. Reinforcement learning

We also carried out experiments on reinforcement learning tasks. Atari 2600 video games[4] consist of various tasks and each task has the same observation shape, which is the size of game screen, but has different sizes of action space, which are the number of controllable lever. From these various tasks, we randomly select eight tasks as follows: $\{StarGunner - Boxing - VideoPinball - Crazyclimber - Gopher - Robotank - DemonAttack - NameThisGame\}$. We choose two baselines, Fine-tuning and EWC, for evaluating our method and train a CNN model, which consists of three convolution layers and one fully connected layer, using PPO[27] on our method and baselines in the exactly same condition. Note that we train a single model with complete continual learning, which means that an agent do not see training data of previous tasks again, unlike [13][28] which learn each task repeatedly during the entire training time. To find the best hyperparameters for baselines, we carried out an extensive search for selecting hyperparameters and we report the results of baselines and our method with the best hyperparameters.

Figure 7 shows the accumulated performance of 8 tasks

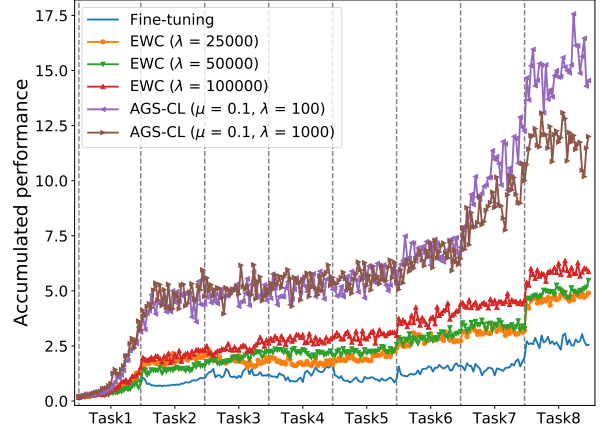


Figure 7. Accumulated performance on Atari tasks.

on baselines and AGS-CL. A reward of tasks for AGS-CL and baselines is normalized with the maximum rewards obtained by Fine-tuning, and then we sum these normalized rewards up to the learned task. In Figure 7, we clearly observe that our method with $\lambda = \{100, 1000\}$ and $\mu = 0.1$ shows superior results compared with baselines. Although EWC also achieves competitive results than Fine-tuning which suffers from catastrophic forgetting, EWC does not reach our performance.

5. Conclusion

We proposed AGS-CL, a new regularization-based method using group sparse regularization. We introduce the loss function with two regularizers for group sparsity and group penalty, and we devised the optimization process with proximal gradient descent that adaptively optimize the regularizations. As the result, AGS-CL significantly outperformed other state-of-the-art baselines in both supervised learning and reinforcement learning.

References

- [1] Hongjoon Ahn, Sungmin Cha, Donggyu Lee, and Taesup Moon. Uncertainty-based continual learning with adaptive regularization. In *Advances in Neural Information Processing Systems*, pages 4394–4404, 2019.
- [2] Rahaf Aljundi, Francesca Babiloni, Mohamed Elhoseiny, Marcus Rohrbach, and Tinne Tuytelaars. Memory aware synapses: Learning what (not) to forget. In *Proceedings of the European Conference on Computer Vision (ECCV)*, pages 139–154, 2018.
- [3] Jose M Alvarez and Mathieu Salzmann. Learning the number of neurons in deep networks. In *Advances in Neural Information Processing Systems*, pages 2270–2278, 2016.
- [4] Greg Brockman, Vicki Cheung, Ludwig Pettersson, Jonas Schneider, John Schulman, Jie Tang, and Wojciech Zaremba. Openai gym. *arXiv preprint arXiv:1606.01540*, 2016.
- [5] Gail A Carpenter and Stephen Grossberg. Art 2: Self-organization of stable category recognition codes for analog input patterns. *Applied Optics*, 26(23):4919–4930, 1987.
- [6] Arslan Chaudhry, Puneet K Dokania, Thalaiyasingam Ajanthan, and Philip HS Torr. Riemannian walk for incremental learning: Understanding forgetting and intransigence. In *Proceedings of the European Conference on Computer Vision (ECCV)*, pages 532–547, 2018.
- [7] Jia Deng, Wei Dong, Richard Socher, Li-Jia Li, Kai Li, and Li Fei-Fei. Imagenet: A large-scale hierarchical image database. In *2009 IEEE conference on computer vision and pattern recognition*, pages 248–255. Ieee, 2009.
- [8] Siavash Golkar, Michael Kagan, and Kyunghyun Cho. Continual learning via neural pruning. *NeurIPS 2019 Neuro AI Workshop*, 2019.
- [9] Kaiming He, Xiangyu Zhang, Shaoqing Ren, and Jian Sun. Deep residual learning for image recognition. In *Proceedings of the IEEE conference on computer vision and pattern recognition*, pages 770–778, 2016.
- [10] Geoffrey Hinton, Oriol Vinyals, and Jeff Dean. Distilling the knowledge in a neural network. *arXiv preprint arXiv:1503.02531*, 2015.
- [11] Ronald Kemker and Christopher Kanan. Fearnnet: Brain-inspired model for incremental learning. In *International Conference on Learning Representations (ICLR)*, 2018.
- [12] Diederik P Kingma and Jimmy Ba. Adam: A method for stochastic optimization. 2014.
- [13] James Kirkpatrick, Razvan Pascanu, Neil Rabinowitz, Joel Veness, Guillaume Desjardins, Andrei A. Rusu, Kieran Milan, John Quan, Tiago Ramalho, Agnieszka Grabska-Barwinska, Demis Hassabis, Claudia Clopath, Dharshan Kumaran, and Raia Hadsell. Overcoming catastrophic forgetting in neural networks. *Proceedings of the National Academy of Sciences*, 114(13):3521–3526, 2017.
- [14] Alex Krizhevsky, Geoffrey Hinton, et al. Learning multiple layers of features from tiny images. 2009.
- [15] Brenden Lake, Ruslan Salakhutdinov, Jason Gross, and Joshua Tenenbaum. One shot learning of simple visual concepts. In *Proceedings of the annual meeting of the cognitive science society*, volume 33, 2011.
- [16] Hao Li, Asim Kadav, Igor Durdanovic, Hanan Samet, and Hans Peter Graf. Pruning filters for efficient convnets. *arXiv preprint arXiv:1608.08710*, 2016.
- [17] Zhizhong Li and Derek Hoiem. Learning without forgetting. *IEEE Transactions on Pattern Analysis and Machine Intelligence*, 40(12):2935–2947, 2017.
- [18] Zhuang Liu, Jianguo Li, Zhiqiang Shen, Gao Huang, Shoumeng Yan, and Changshui Zhang. Learning efficient convolutional networks through network slimming. In *Proceedings of the IEEE International Conference on Computer Vision*, pages 2736–2744, 2017.
- [19] David Lopez-Paz and Marc Aurelio Ranzato. Gradient episodic memory for continual learning. In *Advances in Neural Information Processing System (NIPS)*, pages 6467–6476, 2017.
- [20] Martial Mermillod, Aurélie Bugaiska, and Patrick Bonin. The stability-plasticity dilemma: Investigating the continuum from catastrophic forgetting to age-limited learning effects. *Frontiers in Psychology*, 4:504, 2013.
- [21] Cuong V. Nguyen, Yingzhen Li, Thang D. Bui, and Richard E. Turner. Variational continual learning. In *International Conference on Learning Representations (ICLR)*, 2018.
- [22] Neal Parikh, Stephen Boyd, et al. Proximal algorithms. *Foundations and Trends® in Optimization*, 1(3):127–239, 2014.
- [23] German Ignacio Parisi, Ronald Kemker, Jose L. Part, Christopher Kanan, and Stefan Wermter. Continual lifelong learning with neural networks: A review. *CoRR*, abs/1802.07569, 2018.
- [24] Sylvestre-Alvise Rebuffi, Alexander Kolesnikov, Georg Sperl, and Christoph H Lampert. icarl: Incremental classifier and representation learning. In *Proceedings of the IEEE Conference on Computer Vision and Pattern Recognition (CVPR)*, pages 2001–2010, 2017.
- [25] Andrei A Rusu, Neil C Rabinowitz, Guillaume Desjardins, Hubert Soyer, James Kirkpatrick, Koray Kavukcuoglu, Razvan Pascanu, and Raia Hadsell. Progressive neural networks. *arXiv preprint arXiv:1606.04671*, 2016.
- [26] Simone Scardapane, Danilo Comminiello, Amir Hussain, and Aurelio Uncini. Group sparse regularization for deep neural networks. *Neurocomputing*, 241:81–89, 2017.
- [27] John Schulman, Filip Wolski, Prafulla Dhariwal, Alec Radford, and Oleg Klimov. Proximal policy optimization algorithms. *arXiv preprint arXiv:1707.06347*, 2017.
- [28] Jonathan Schwarz, Wojciech Czarnecki, Jelena Luketina, Agnieszka Grabska-Barwinska, Yee Whye Teh, Razvan Pascanu, and Raia Hadsell. Progress & compress: A scalable framework for continual learning. In *International Conference on Machine Learning (ICML)*, pages 4528–4537, 2018.
- [29] Joan Serra, Didac Suris, Marius Miron, and Alexandros Karatzoglou. Overcoming catastrophic forgetting with hard attention to the task. *arXiv preprint arXiv:1801.01423*, 2018.
- [30] Hanul Shin, Jung Kwon Lee, Jaehong Kim, and Jiwon Kim. Continual learning with deep generative replay. In *Advances in Neural Information Processing System (NIPS)*, pages 2990–2999, 2017.
- [31] Hansheng Wang and Chenlei Leng. A note on adaptive group lasso. *Computational statistics & data analysis*, 52(12):5277–5286, 2008.

- [32] Peter Welinder, Steve Branson, Takeshi Mita, Catherine Wah, Florian Schroff, Serge Belongie, and Pietro Perona. Caltech-ucsd birds 200. 2010.
- [33] Wei Wen, Chunpeng Wu, Yandan Wang, Yiran Chen, and Hai Li. Learning structured sparsity in deep neural networks. In *Advances in neural information processing systems*, pages 2074–2082, 2016.
- [34] Jaehong Yoon and Sung Ju Hwang. Combined group and exclusive sparsity for deep neural networks. In *Proceedings of the 34th International Conference on Machine Learning-Volume 70*, pages 3958–3966. JMLR. org, 2017.
- [35] Jaehong Yoon, Eunho Yang, Jeongtae Lee, and Sung Ju Hwang. Lifelong learning with dynamically expandable networks. In *International Conference on Learning Representations (ICLR)*, 2018.
- [36] Friedemann Zenke, Ben Poole, and Surya Ganguli. Continual learning through synaptic intelligence. In *International Conference on Machine Learning (ICML)*, pages 3987–3995, 2017.
- [37] Zhuangwei Zhuang, Mingkui Tan, Bohan Zhuang, Jing Liu, Yong Guo, Qingyao Wu, Junzhou Huang, and Jinhui Zhu. Discrimination-aware channel pruning for deep neural networks. In *Advances in Neural Information Processing Systems*, pages 875–886, 2018.
- [38] H. Zou. The adaptive Lasso and its oracle properties. *Journal of the American Statistical Association*, 101:1418–1429, 2006.